0.3-dB-Loss SCF-to-MCF Power Splitter Based on a Biconical Splice Taper

Sijing Liang(1), John D. Downie(2), Sergejs Makovejs(3), Periklis Petropoulos(1), Yongmin Jung(1)

(1) Optoelectronics Research Centre, University of Southampton, Southampton, SO17 1BJ, UK, s.liang@soton.ac.uk
(2) Corning Research and Development Corp., 1 Riverfront Plaza, Corning, NY 14831, USA
(3) Corning Incorporated, Corning Optical Communications, Lakeside Business Village, CH5 3XD, UK

Abstract *We present a low-loss SCF-to-MCF power splitter based on a biconical splice taper. Power distribution uniformity is enhanced through a macrobending-based post-processing technique that compensates for MCF core inhomogeneity, enabling precise output balancing without additional loss and improving the practicality of scalable splitter designs. ©2025 The Author(s)*

Introduction

Single-core fibre (SCF) to multicore fibre (MCF) power splitters, which distribute optical power from an SCF into multiple output cores of an MCF, are attracting growing interest in a range of applications, including optical fibre amplifiers, fibre lasers and distributed sensing systems [1-3]. Compared to conventional fanout devices, SCF-to-MCF power splitters offer a more compact footprint, improved integration, and higher energy efficiency. These advantages make them particularly suitable for delivering pump power to core-pumped MCF amplifiers [1], embedding into compact fibre laser architecture [2], and enabling multi-point signal collection in fibre-optic sensor networks [3].

Among the various implementation techniques proposed to date [4-10], the splice taper method – where a biconical taper is formed at the splice point between an SCF and an MCF – has emerged as a promising solution [8-10]. Unlike solutions requiring custom-made fibres (e.g., polygon-shape core fibres [4,5] or multicore photonic crystal fibre structures [6]), the splice taper approach leverages standard fibre geometries and offers significant advantages in terms of fabrication simplicity, reproducibility, and cost-effectiveness. Additionally, it avoids the complexity and equipment overhead associated with methods such as ultrafast laser inscription [7].

Despite its potential, the widespread adoption of splice-taper-based SCF-to-MCF power splitters has been limited by two major technical challenges: high insertion loss (IL) and poor power uniformity across MCF cores. While simulations frequently predict ILs below 0.5 dB, experimental implementations often exhibit losses exceeding 2 dB [8-10], primarily due to fabrication tolerances and suboptimal taper designs. Moreover, significant power imbalance across MCF cores – often greater than 50% – is commonly observed, with limited understanding of the root causes [8-10].

In this paper, we demonstrate a low-loss SCF-to-MCF power splitter based on a precisely fabricated biconical splice taper. By carefully designing and optimizing the taper parameters, we achieve a record-low IL of 0.3 dB. Furthermore, to address the core-to-core power imbalance issue, we introduce a macrobending-based post-processing technique that effectively compensates for MCF core inhomogeneity, reducing power imbalance to below 10% without introducing additional loss. Our results validate the viability of the splice-taper-based SCF-to-MCF power splitter as a manufacturable solution scalable to a wide range of MCF designs.

Spice Taper Design and Fabrication

Figure 1 shows the structure of the SCF-to-MCF power splitter which comprises an input SCF, an output MCF, and a symmetric biconical taper centered at the splice junction. The operating principle is illustrated by the mode evolution in Fig. 2. The fundamental LP_{01} core mode (LP_{01}^{Co})

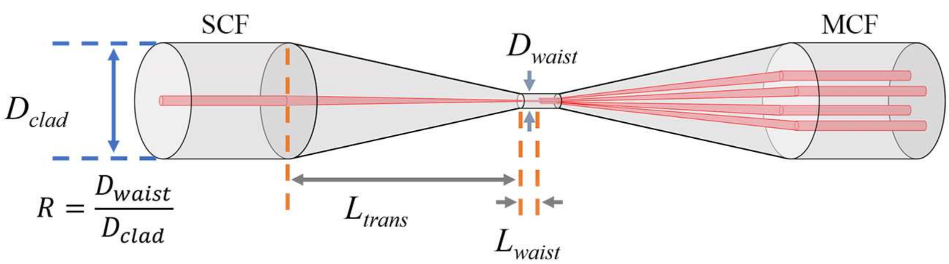

Fig. 1: Schematic of the SCF-to-MCF power splitter based on a biconical splice taper.

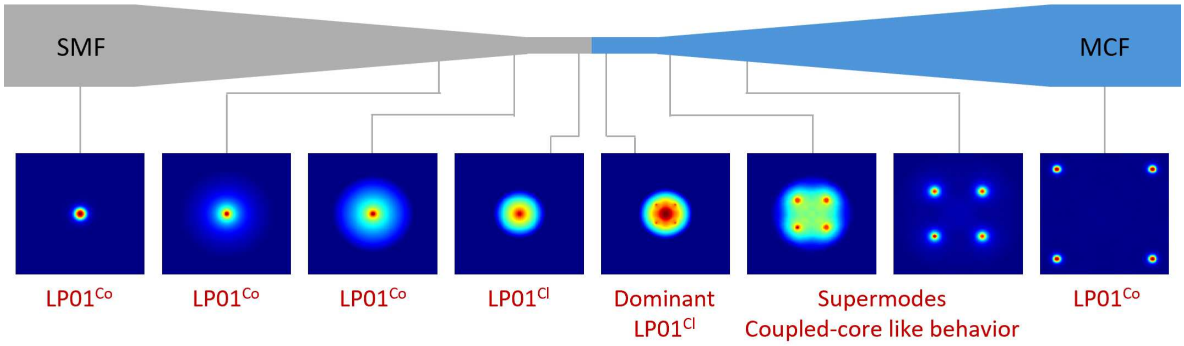

Fig. 2: Calculated transverse field profiles at various positions along the SMF-MCF splice taper.

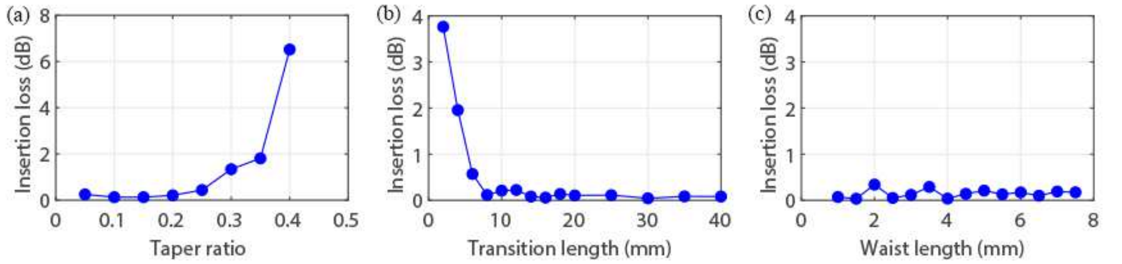

Fig. 3: Calculated insertion loss of the power splitter as a function of (a) taper ratio, (b) transition length and (c) waist length.

of the SCF is adiabatically transformed into a cladding-guided mode (LP_{01}^{Cl}) within the taper waist. The LP_{01}^{Cl} mode, governed primarily by the cladding/air interface and largely unaffected by the presence of the tapered core structures in SCF and MCF, propagates through the splice joint with minimal optical loss, thanks to the matched cladding diameters of the SCF and MCF. In the subsequent up-taper region, the expanding cores of the MCF adiabatically recapture the cladding-guided light, and the LP_{01}^{Cl} mode evolves into a symmetric LP_{01} supermode. This process results in efficient and balanced power redistribution across all output cores.

The taper geometry is characterized by four key parameters: waist diameter (D_{waist}), waist length (L_{waist}), taper transition length (L_{trans}), and taper ratio R ($R=D_{waist}/D_{clad}$). These parameters were optimized for our demonstration using a 4-core MCF (4CF) designed for 980 nm operation. The 4CF has core/cladding diameters of 3.3/125 μm, a core NA of 0.21, and a core pitch of 44.2 μm. The input SCF has core/cladding diameters of 5.3/125 μm and an NA of 0.14, ensuring single-mode operation. In both simulations and fabrication, linear taper profiles were assumed, with the 4CF modeled as having ideal core homogeneity.

Beam propagation method (BPM) simulations were carried out to evaluate IL as a function of taper parameters (Fig. 3). Note that IL of the power splitter is defined as the ratio of the total output power from all cores of the MCF to the power at the input of the SCF. The results indicate that IL<0.5 dB can be achieved when the taper ratio R≤0.25 and the transition length L_{trans}>6 mm. Under these optimized conditions, the core diameters of the SCF and 4CF are reduced to <1.35 μm and <0.85 μm, respectively, and the 4CF core pitch contracts to ≤11.05 μm. While simulations suggest that the waist length L_{waist} has a minimal impact on IL, a longer waist length can improve fabrication tolerance and alignment accuracy during taper formation.

The splice taper fabrication was performed using a Fujikura ARCMaster FSM-100P+ splicer capable of producing precise and replicable tapers up to 18 mm in length. The final taper was fabricated using the optimized parameters: R = 0.2, L_{waist} = 1 mm, and L_{trans} = 8 mm. After fine-tuning the arc power, duration, and taper speed, the fabricated taper achieved a measured IL of 0.3 dB, just slightly higher than the 0.2-dB loss predicted by simulation. A microscopic image of the taper waist is shown in Fig. 4(a). The far-field beam image in Fig. 4(b) reveals a normalized core power ratio of 1:0.94:0.9:0.76, yielding a power imbalance, defined as the power difference between the highest and lowest core power, of 24%. This deviation from simulations is attributed to non-ideal homogeneity in the actual 4CF, such as slight variations in core diameter and/or core refractive index (RI).

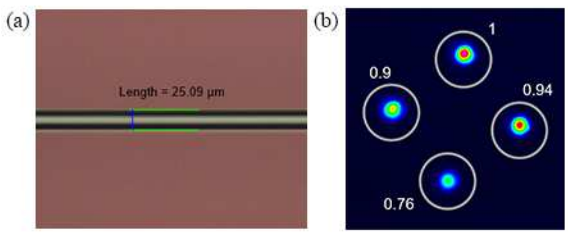

Fig. 4: (a) Microscopic image of the taper waist; (b) output beam image captured by a CCD camera.

Post-processing for Improved Core Power Uniformity

Figure 5 presents simulation results illustrating the impact of MCF inhomogeneity on output power distribution. In Fig. 5(a), a single core (core #4) has a slightly higher RI than the other cores, while maintaining identical core diameters. A small RI difference of 1×10^{-3} can result in a power imbalance of up to 25%. RI measurements on our 4CF confirmed the presence of such variations. Similar power imbalances were also observed in simulations assuming inhomogeneous core diameters. Fig. 5(b) summarizes the power imbalances induced by percentage changes in RI and core diameter, respectively. The results show that variations in core diameter have a more pronounced effect on power imbalance, indicating a higher sensitivity to geometric inhomogeneity. Although these inhomogeneities have negligible impact on IL as shown in Fig. 5(c), they significantly degrade power uniformity – highlighting the importance of core homogeneity in the power splitter performance. To mitigate this requirement, we introduced a post-processing method based on macrobending. This method leverages the sensitivity of each core's effective RI to controlled bending, thereby altering the modal distribution and supermode transitions within the tapered region [11]. Consequently, by fine-tuning the bending conditions, we can achieve precise control over power redistribution among MCF cores.

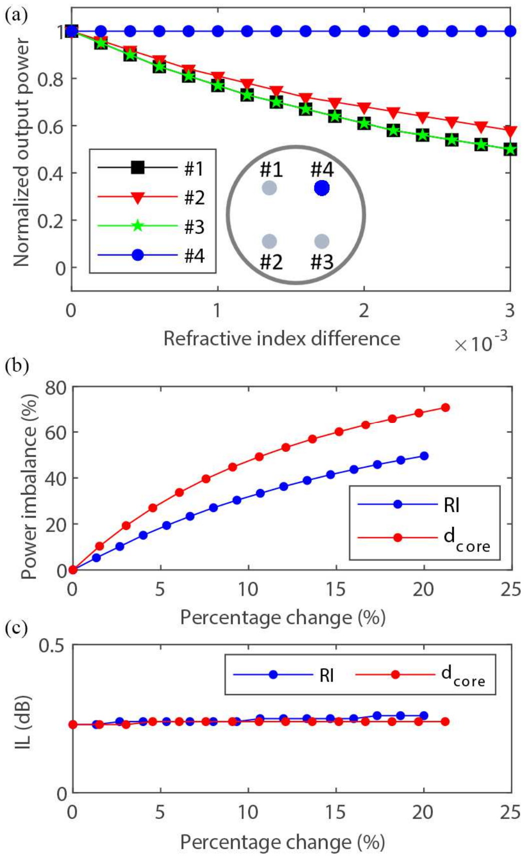

Fig. 5: Simulated impact of MCF core inhomogeneity on power distribution uniformity and IL.

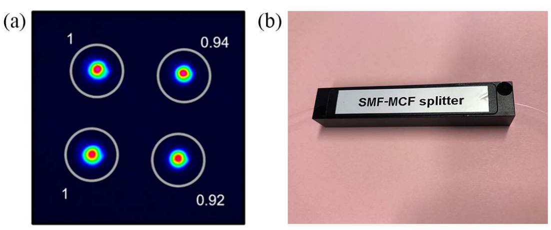

Fig. 6: (a) Improved core power uniformity after post-processing; (b) photo of the packaged power splitter.

A custom experimental setup was developed in-house using 3-axis translation stages and fibre rotators to precisely adjust the bending direction and strength. With real-time monitoring of the far-field output pattern, the macrobending conditions were optimized to minimize power imbalance. After post-processing, the normalized output core powers improved significantly to 1:1:0.94:0.92, while maintaining the same IL of 0.3 dB. The final device was secured and packaged with the optimized bend geometry fixed within a protective case to ensure long-term mechanical stability. The post-processed output beam profile and the packaged power splitter are shown in Fig. 6, respectively.

Conclusions

We have designed and demonstrated a high-performance SCF-to-MCF power splitter based on a biconical splice taper, achieving a record-low insertion loss of 0.3 dB and excellent power uniformity with less than 10% variance across MCF cores. To address core-to-core power imbalance caused by MCF inhomogeneity, we introduced a macrobending-based post-processing technique that enables precise adjustment of output power distribution without introducing additional loss. This method significantly reduces the reliance on highly homogeneous MCFs, thereby enhancing the practicality, scalability, and manufacturability of splice-taper-based SCF-to-MCF power splitters for applications in multicore fibre amplifiers, fibre lasers, and distributed sensing systems.

Acknowledgements

The work of Sijing Liang and Periklis Petropoulos was partly supported by the Engineering and Physical Science Research Council under Grant EP/X04047X/1.

References

[1] S. Liang, J. D. Downie, S. Makovejs, I. A. Davidson, N. Choudhury, Z. Kakaei, J. Sahu, P. Petropoulos, and Y. Jung, "Novel Core-pumped Multicore Fiber Amplifier Integrated with Energy-efficient Pump Light Distributor," presented at *Optical Fiber Communication Conference (OFC)*, San Francisco, USA, 2025, W4J.4.

[2] Y. Jung, N. Vukovic, C. A. Codemard, and M. N. Zervas, "Multispot fiber lasers for material processing applications," in *Proc. SPIE 12865, Fiber Lasers XXI: Technology and Systems*, San Francisco, USA, 2024, 128650B. DOI: 10.1117/12.3000216

[3] Z. Zhang, A. Rahman, J. Fiebrandt, Y. Wang, K. Sun, J. Luo, K. Madhav, and M.M. Roth, "Fiber Vector Sensor Based on Multimode Interference and Image Tapping", *Sensors*, vol. 19, no. 2, 321, 2019. DOI: 10.3390/s19020321

[4] S. Liang, J. D. Downie, S. Makovejs, M. Edwards, P. Petropoulos, and Y. Jung, "Efficient SMF-to-MCF Power Splitter Using Multimode Interference in Square Core Fiber", presented at *Optical Fiber Communication Conference (OFC)*, San Francisco, USA, 2025, W4J.2.

[5] Z. Zhang, J. Fiebrandt, D. Haynes, Y. Wang, K. Sun, K. Madhav, and M. M. Roth, "Single-Mode to 61 Spots Divider With Multimode Interference in Hexagonal Core Fiber," *Photonics Technology Letters*, vol. 30, no. 14, pp. 1337-1340, 2018. DOI: 10.1109/LPT.2018.2847233.

[6] S. K. Varshney, K. Saitoh, R. K. Sinha, and M. Koshiba, "Coupling Characteristics of Multicore Photonic Crystal Fiber-Based 1 x 4 Power Splitters," *Journal of Lightwave Technology*, vol. 27, no. 12, pp. 2062-2068, 2009. DOI: 10.1109/JLT.2008.2006692

[7] T. Baghdasaryan, K. Vanmol, H. Thienpont, F. Berghmans, and J. V. Erps, "Ultracompact 3D splitter for Single-Core to Multi-Core Optical Fiber Connections Fabricated Through Direct Laser Writing in Polymer", *Laser & Photonics Reviews*, vol. 18, no. 11, 2400089, 2024. DOI: 10.1002/lpor.202400089

[8] L. Yuan, Z. Liu, and J. Yang, "Coupling characteristics between single-core fiber and multicore fiber", *Optics Letters*, vol. 31, no. 22, pp. 3237-3239, 2006. DOI: 10.1364/OL.31.003237

[9] L. Yuan, Z. Liu, J. Yang, and C. Guan, "Bitapered fiber coupling characteristics between single-mode single-core fiber and single-mode multicore fiber," *Applied Optics*, vol. 47, no. 18, pp. 3307-3312, 2008. DOI: 10.1364/AO.47.003307

[10] A. Pytel, M. Napierała, Ł. Szostkiewicz, Ł. Ostrowski, M. Murawski, P. Mergo, and T. Nasiłowski, "Optical power 1×7 splitter based on multicore fiber technology", *Optical Fiber Technology*, vol. 37, pp.1-5, 2017. DOI: 10.1016/j.yofte.2017.06.002

[11] T. Sakamoto, T. Mori, M. Wada, T. Yamamoto, F. Yamamoto and K. Nakajima, "Fiber Twisting- and Bending-Induced Adiabatic/Nonadiabatic Super-Mode Transition in Coupled Multicore Fiber," *Journal of Lightwave Technology*, vol. 34, no. 4, pp. 1228-1237, 2016. DOI: 10.1109/JLT.2015.2502260